Erciyes Üniversitesi
Fen Bilimleri Dergisi
2, 195-210, (1986)

FORMATION OF Nb_3Sn LAYER IN MULTIFLEMENTARY SUPERCONDUCTING WIRES

Yusuf S. HASÇİÇEK

Erciyes Üniversitesi, Fen-Edebiyat Fakültesi, Fizik Bölümü, KAYSERİ

SUMMARY

The formation of Nb_3Sn in a so-called diffusion comple, thermodynamics of the proces, and layer growth in the bronze processed multifilamentary superconducting Nb_3Sn wires were briefly discussed.

ÇOK FİLEMENTLİ SÜPERİLETKEN TELLERDE Nb_3Sn TABAKASININ OLUŞMASI

ÖZET

Bir difüsyon çiftinde Nb_3Sn oluşması, meselenin termodinamiği ve bronz metodu ile üretilen çok filementli süperiletken Nb_3Sn tellerinde tabaka büyümesi kısaca tartışıldı.

1. INTRODUCTION

Superconductors are used wherever stable or large, both in strength and volume, magnetic fields are in demand. Hard superconductors have much superior critical properties (J_c, T_c, H_{c2}) than the other ones. Actually Nb_3Sn and V_3Ga are those superconductors which can be produced in long lengths which is necessary for applications. Fabrication of superconducting wires, namely "bronze route" was discussed in a previons paper [1] here the formation of Nb_3Sn layer at the interface of Nb core and Cu-Sn matrix is briefly discussed.

2. THERMODYNAMICS OF THE PROCESS

It is well established that the interfacial structure at a diffusion couple between two elements is composed exclusively of single phases appearing in the compositional sequence in which corresponding phases appear according to the appropriate phase diagrams [2] . In multicomponent systems, the only phases which will form in these diffusion couples are those phases whose phase fields lie on the composition (or diffusion)

path connecting the two initial components of the couple [2, 3] . These phases also appear to be those which have higher stability. Before considering the Nb_3Sn case (the "bronze process"), the Nb-Sn diffusion couple will be discussed.

Commercial Nb_3Sn tape conductors have been produced for many years by heating Nb or (Nb-1 at % Zr) tapes in a tin bath above 930^oC [4, 7] . When the bath temperature is above 930^oC single-phase Nb_3Sn layers are formed, but when lower than this other non-superconducting compounds are dominant at the interface. This difference is readily understood from the Nb-Sn phase diagram. The Nb-Sn phase diagram due to Charlesworth et al [4] is shown in Fig.1. From this diagram the only stable phase above 930^oC is Nb_3Sn. However at temperatures below 930^oC two other phases Nb_6Sn_5 and $NbSn_2$ are also stable, and all these phases will grow at the interface. The relative thickness of the compound layers is primarily determined by the kinetics of growth. In this particular system, the $NbSn_2$ phase is most easily formed, while the Nb_3Sn layer is the slowest growth layer. However, if the composition of mixture is Nb-25 at % Sn, the composite should eventually become totally Nb_3Sn since Nb_3Sn is the most stable phase in this system. But the time scale involved is not practical for most cases.

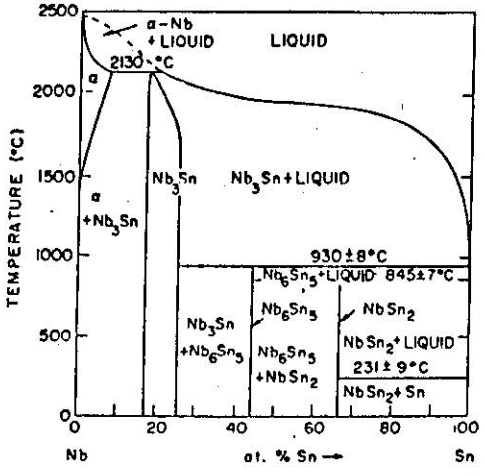

Fig.1 : Nb-Sn binary phase diagram, due to Charlesworth et al [4]

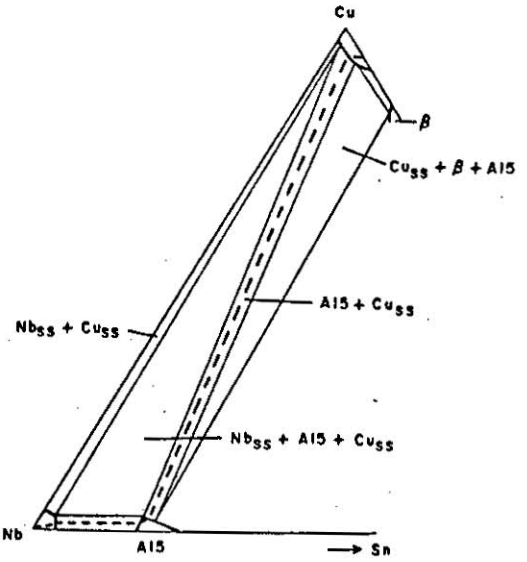

Fig.2 : Part of the Nb-Cu-Sn ternary isotherm at about 700°C. The dashed line represents the solid state diffusion path between Cu-Sn solid solution and pure niobium (from Dew-Hughes and Luhman [9])

As referred to above the terminating phase is determined by the relative thermodyanamic stability. Raynor [5] introduced the stability index (S.I) as a measure of the relative stability of the phases which have the same two terminal elements (phases). This index provides a very convenient, practical approach to the probability of the appearance of the phases in a diffusion couple. The stability index for a binary compound of the form $A_x B_{(1-x)}$ is defined as [13]

$$S.I. = T_m / [\, T_B + (T_A - T_B)\,(1 - X_B)\,] \qquad (1)$$

where T_m, T_A, T_B are the melting temperature of the compound and of the elements A and B respectively and X_B is the atomic fraction of element B in the compound. This equation indicates that those compounds for which the melting points are above the line drawn between the melting points for the elements A and B are more stable than those with the melting temperatures below it. There are other indices such as the

formation temperature ratio (F.T.R.) introduced by Hartsough [6] and later Luhman, Horigami and Dew-Hughes [3] modified the stability index for the bronze route composites which give some insight as to why some of the A15 phases would not be formed by the bronze route. They substituted the melting points of the starting solid solutions in place of the melting temperatures of the two elements forming the compound.

For a better understanding of the formation of Nb_3Sn in the bronze route composites one has to consider the Nb-Cu-Sn ternary isotherm at the reaction temperature. Fortunately the useful portion of this ternary phase diagram is available due to Hopkins et al [8] . Dew-Hughes et al [9] constructed part of this ternary diagram at about 700°C and this is shown in Fig.2. As seen in the figure the solid state diffusion path (dashed line) goes through the A15 phase only between Nb and Cu-Sn solid solution, and the S.I. of Nb_3Sn is greater than one [9, 10, 13] . Therefore the only stable phase in this system at about 700°C is the A15 Nb_3Sn. Experimental results by many workers have shown this to be so. The Nb_3Sn layer growt and grain growth will be dealt with in the following sections.

3. Nb_3Sn LAYER GROWTH

In this section the kinetics for the growth of the Nb_3Sn compound layer at the interface of the Nb core and the matrix (Cu-Sn) in the bronze processed wires are examined using a representative diffusion couple. As yet no one has attempted to solve the diffusion equations with the exact initial boundary conditions for the real case in the bronze route. First the basic diffusion equations pertinent to the growth are considered to derive an expression for the growth of the Nb_3Sn layer [11, 13] . Some deviation of the experimental results from the usual parabolic growth law [14, 16] (and many others), led to the consideration of another mechanism which is grain boundary diffusion of Sn through the Nb_3Sn layer [16, 18] . A summary of this mechanisms is also given later in this section.

3.1. GROWTH MECHANISM BY BULK DIFFUSION

Suenaga gave the most recent review on this subject in a neat way [13]. To simplify the problem he constructed a pseudobinary phase diagram for Nb-(Cu-Sn) from the Nb-Cu-Sn ternary isotherm (see Fig.3). Since the composition (or diffusion) path at about 700°C of the Nb-Cu-Sn isotherm between Nb and (Cu-Sn) goes directly through the A15 phase a schematic pseudobinary phase diagram can be constructed. The dashed line in the figure shows the diffusion path at about 700°C between Nb and (Cu-Sn). The diffusion of Sn through Nb_3Sn can be considered from two points of view. One is the concentration approach, the other is the chemical potential approach. Only the concentration approach is given here.

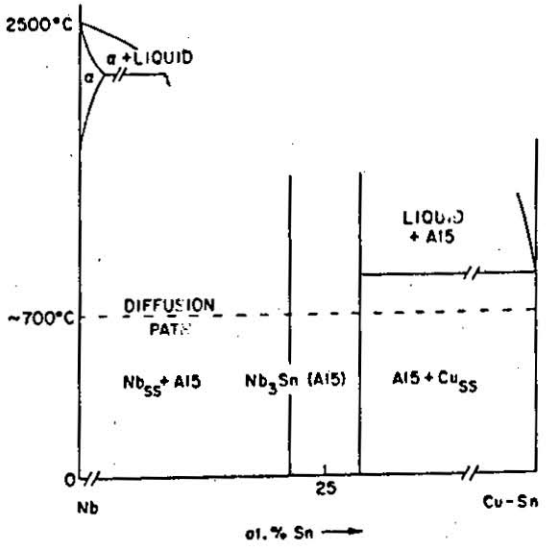

Fig.3 : Schematic psuedo-binary phase diagram for the Nb-(Cu-Sn) system for the Nb-(Cu-Sn) diffusion couple (from M. Suenaga [13]).

In Fig.4 a planar diffusion couple is shown together with the relative Sn concentration in different regions. As mentioned above Sn is the only substance diffusing through Nb_3Sn. Assuming that the formation of the Nb_3Sn compound takes place at the left interface, V_f is the volume of Nb_3Sn formed per atom of Sn, J_{sn} is the tin flux arriving at the left

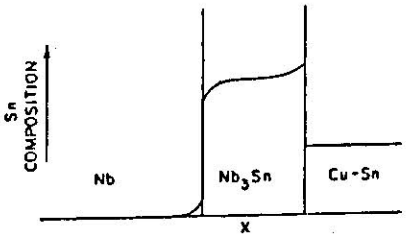

Fig.4 : Schematic diagram of the Sn concentration in the Nb-Nb_3Sn (Cu-Sn) diffusion couple (After M. Suenaga [13]).

interface, and X is the layer thickness, the Nb_3Sn layer growth rate can be written as

$$(dX/dt) = J_{sn}\, V_f \qquad (2)$$

For a constant layer thickness the flux is given by Fick's law as

$$J_{sn} = D\,(dC/dX)\,|_{Nb\text{-}Nb_3Sn} \cong D\,(\Delta C/X) \qquad (3)$$

where D is the diffusion coefficient of Sn in the Nb_3Sn layer, and ΔC is the difference in Sn concentration across the layer at a given temperature. It is important to state here that the Nb-Nb_3Sn interface is moving. As mentioned above the exact equation for J_{sn} with all the initial boundary conditions is almost intractable. Bu the form

$$J_{sn} = (\alpha D \Delta C)/X \qquad (4)$$

is convenient, because the usual parabolic law can b 'erived from this. $\alpha = 1$ for stationary interfaces. It is also likely at $\alpha < 1$ for this case [13] .

From equation (2) and (4) the growth-rate equation car. ɔe derived as

$$X^2 = 2\,\alpha D\,\Delta C V_f\, t \qquad (5)$$

or

$$X = K\, t^{1/2} \tag{6}$$

This is the classical parabolic growth law since $K = (2\alpha\, D\, \Delta C V_f)^{1/2}$ is most likely to be constant with time and a function of reaction temperature.

The Nb_3Sn layer growth as a function of time and temperature can be expressed as

$$X = A\,(t) \exp\,(-\,Q_L/RT) \tag{7}$$

where X : layer thickness, Q_L : activation energy for layer growth, T : absolute temperature [17] .

3.2. GROWTH MECHANISM BY GRAIN BOUNDARY DIFFUSION

A detailed description of this mechanism is given by Farrel et al [17] based on Whipple's formulation [26, 27] . A summary of their formulation is given below.

After observing a slower growth rate than the parabolic growth they considered possible mechanisms which will result in slower growth rate. Grain boundary diffusion is known to be faster than normal bulk diffusion [27, 28] . But if there is an appreciable grain growth with time this is likely to slow the growth. This was the approach to the grain boundary diffusion controlled growth rate.

In Whipple's formulation [26] , the diffusion in a system containing a signle high diffusivity slab of a width 2a in a semi-infinite medium is described by the equation

$$D \nabla^2 C = \frac{\partial C}{\partial t} \tag{8}$$

in the bulk of the medium, and

$$D' \frac{\partial^2 C}{\partial x^2} + \frac{D}{a} \frac{\partial C}{\partial y} = \frac{\partial C}{\partial t} \qquad \text{at} \quad x = 0 \qquad (9)$$

at the slab. Where D' is the diffusion coefficient in the slab representing the grain boundary. Fig.5 shows the geometry. Calculations [17, 26] using this model indicate that the equi-concentration contours advance with a time dependence less than the parabolic law under certain conditions in the absence of compound formation. This is primarily due to the leakage of flux into the bulk of the grain. But, when compound formation takes place at the interface, almost all the flux will be carried to the growth interface and very little is lost to the bulk of the grains. In fact, in most cases, the concentration in the grain boundary approaches steady-state conditions because the motion of the growth front is slower than that of diffusion of atoms at the grain boundaries. Thus it is expected that a growth interface fed by grain boundary diffusion will lead to a parabolic time dependence of the layer thickness [13] .

The possibility of nonparabolic growth controlled by the grain boundary diffusion was investigated by Farrell et al [17] . They showed that the growth would be less than the parabolic one, if the Sn concentration at the Nb-Nb_3Sn interface was much less than 18 at % or if there was significant leakage of Sn into the bulk of the grains, by considering a fixed array of grain boundaries in the Nb_3Sn layer perpendicular to the growth interface. This was unrealistic and they concluded that when compound formation is controlled by a simple grain-boundary diffusion through a fixed array of grain boundaries, the growth of the layer will follow a parabolic law. These authors showed that the growth will be slower than the parabolic one if there is appreciable grain growth in the Nb_3Sn layer. This reduces the total high-diffusivity path area with time, and in turn the flux arriving at the growth interface will also decrease with time. A summary of their formulation is given below.

The grain boundary flux through a series of parallel equidistant boundaries causes the layer thickness X to increase at a rate obtained from the conservation equation

$$\bar{L} C_1 (dX/dt) = 2aD' (C_0/X) \quad (10)$$

more generally (considering the grain shape effect)

$$\gamma \bar{L}^2 C_1 (dX/dt) = a\bar{L} D' (C_0/X) \quad (11)$$

where $(a\bar{L})/(\gamma\bar{L}^2)$ is the fraction of the area of the interface occupied by the grain boundaries, γ is a geometrical factor depending on the shape of the grains, C_1 is the concentration of Sn at the growth interface C_0 is the Sn concentration at the original interface ($C_0 > C_1$). Equation (11) may be integrated to yield

$$X^2 = [(2 C_0 a D')/(C_1 \gamma)] \int_0^t (\bar{L}/\bar{L}^2) dt \quad (12)$$

$$X = \{ (2 C_0 a D')/[(1 - m) C_1 \gamma \lambda_0 (T)] \}^{1/2} t^{1/2(1-m)} \quad (13)$$

where it is assumed that $\bar{L}^2 / \bar{L} = \lambda_0 (T) t^m$ and $\lambda_0 (T)$ is a temperature dependent coefficient and m is determined by the relative values of activation energies for grain boundary diffusion and grain growth. For m values larger than zero the growth rate will be less than parabolic. The authors also showed that the effect of the grain growth in their particular case was a significant factor in slowing the growth process.

In all these studies, when the layer growth was examined the phosphorus content of the matrix, the depletion of Sn, the effect of the shape of the filaments, the effect of a high concentration of vacancies around Nb_3Sn layer in the matrix were never considered. And on top of these when a fourth element was added, to the Nb-Cu-Sn ternary, to the matrix or the core the conditions were thought to be the same as those in the ternary case [48] .

Reddi et al [29] considered different rate controlling factors, for Sn diffusion through matrix and Sn diffusion through the Nb_3Sn layer and found values for n ($X = A(T) t^n$) ranging between 0.25 and 1. The experimental results of Kwasnitza et al [30] above consideration

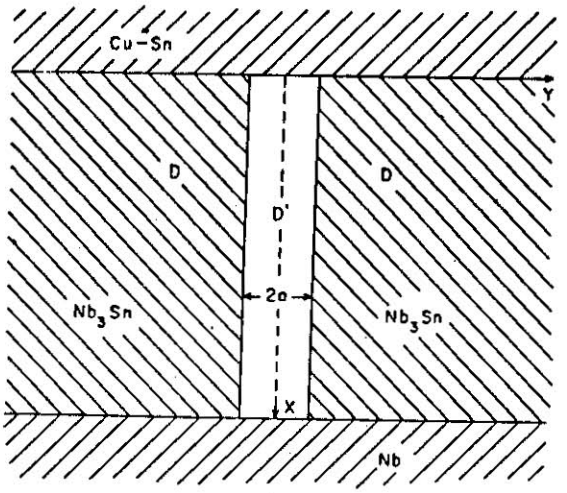

Fig.5 : Schematic representation of a Nb_3Sn layer containing a grain boundary (from Farrell et al. [17])

favoured the Sn diffusion through the Nb_3Sn layer as rate controlling.

4. GRAIN GROWTH in the Nb_3Sn LAYER

A full description of grain growth is beyond the scope of this paper. A brief description of grain growth in general and a few examples of the results on Nb_3Sn are given below.

In the general sense normal grain growth starts after the completion of the primary recrystallization of a deformed metal. And in the absence of inclusions and secondary particles grain growth at a constant temperature can be expressed as :

$$(dD/dt) = K' [(1/D) - (1/D_m)] \qquad (14)$$

where D is the average grain size, D_m is the maximum grain size attainable at the temperature of the observation, K' is constant of time and a function of temperature, t is time. By integrating equation (14) the expression for the average grain size is achieved as :

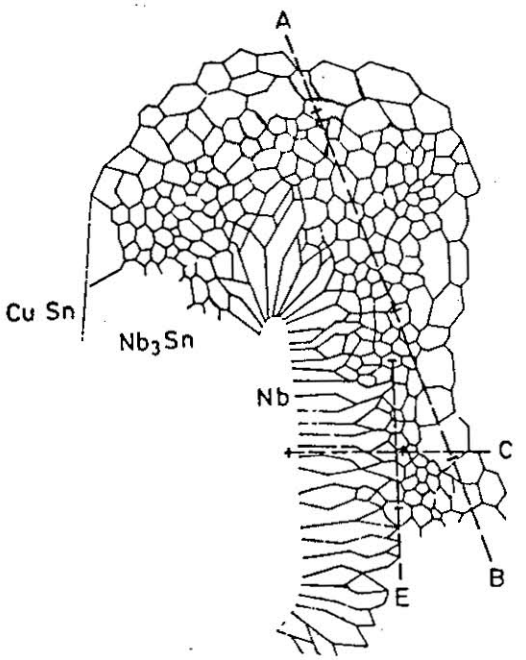

Fig.6 : Sketch grain structure of the Nb_3Sn layer in the bronze processed wires built up from TEM observations made on longitudinal specimens (from Schelb [44]). Although this is the closest sketch to the true grain structure, there is neither a continuous equiaxed large grained layer throughout the periphery of the filament, nor a continuous columnar grained inner layer in the TEM micrographs taken from transverse specimens [45, 48] .

$$[(D_o-D)/D_m] + \ln [(D_m - D_o)/(D_m - D)] = (K'/D_m^2)\, t \qquad (15)$$

where D_o is the initial grain size at the onset of the grain growth. As mentioned above K' is a function of temperature as

$$K' = K \exp (-Q_G/RT) \qquad (16)$$

where K is a constant, Q_G is the activation energy for grain growth R is the universal gas constant, T is temperature. Therefore, the expression for the average grain size in a general grain growth process can be written as :

$$[(D_o-D)/D_m] + \ln [(D_m-D_o)/(D_m-D)] = (K/D_m^2)\, t \exp (-Q_G/RT) \qquad (17)$$

The above formalism is due to Burke et al [31] and others [32, 34] .

It was known that grain boundaries and second phase particles were possible flux pinning centres in commercial V_3Ga and Nb_3Sn tapes [35, 38] . Actually it was common practice to add inclusions of ZrO_2 to commercial tapes, but it was not clear whether inclusions acted as a control in grain growth or actually as the flux pinning centres.

The first grain size measurements in "bronze processed" Nb_3Sn layer is due to Scanlan et al [31] . They used longitudinal sections from tape specimens prepared by both the bronze route and commercial tape (chemical vapour deposition or liquid-diffusion). They concluded that grain growth was parabolic at a given temperature and pinning was mainly by the grain boundaries. Several others have followed using Scanning Electron Microscopy [40, 41] , and Transmission Electron Microscopy [35, 39, 42, 44] . In general SEM results on grain sizes are higher than TEM results especially in the early stages of growth. Among these West and Rawlings [42] and Schelb [44] are the most extensive ones, although their results are based on the micrographs taken from longitudinal sections. West and Rawlings concluded that the Nb_3Sn grains are equiaxed and large at the periphery of the filaments and they get smaller and columnar towards the centre of the filaments at normal reaction temperatures (about $700^{o}C$). They also observed the very fine grained Nb_3Sn layer around the filaments before the final reaction which forms during intermediate annealings in the bronze process.

Schelb [44] carried out one of the most recent TEM work on multifilamentary bronze processed Nb_3Sn. His results are based again on micrographs taken from longitudinal sections. Nevertheless he sketched a grain structure for Nb_3Sn which is closer to the actual grain morphology of the layers observed in transverse sections [45, 48] , see also Fig.6. This is one of the recent works which concentrate both on the grain growth in the Nb_3Sn layer grown by the bronze process and the effect of grain size on the critical parameters. His results on the measurements of the grain size best fit the expression which can be written as (based on Burke and Turnbull [31] .

$$d = \{ d_m - (d_m - d_o) \exp [- (M/\bar{d}_m^2) t_R - (d-d_o)/d_m] \} \exp (-Q_G/RT_R) \quad (18)$$

where d is the average grain size, d_m is the maximum grain size attainable at the reaction temperature, d_o is the initial grain size, M is the grain boundary mobility, t_R and T_R are the time and temperature of the reaction respectively. He also extrapolated expressions for d_m and d_o for varying reaction temperatures which are

$$d_m = 2.59\ 10^5 \exp (-Q_G/RT_R) \quad (19)$$

$$d_o = 1.58\ 10^5 \exp (-Q_G/RT_R) \quad (20)$$

where Q_G is 63 $\mp$ 2 KJ/mole.

The most recent and extensive work on the layer growth and on the microstructure of this layer was carried out by Hasçiçek et al [45, 48] . Hasçiçek reacted the 5143 filament wires for varying times at 650°C, 700°C, 850°C and at 700°C after 15 minutes at 850°C. He measured the Nb_3Sn layer thickness of over one hundred filaments from each set by using a digitizer [48] .

Hasçiçek [48, 50] also reacted a set of short lengths of wires at 700°C and another set at 850°C to grow the same layer thickness but having different grain sizes. These sets were then reacted at 700°C for varying times. The equality of the layer thickness and the grain structure of the layers were demonstarated by optical microscopy, electron microscopy and electron microprobe [48] .

Hasçiçek [48] presented vast samples of Nb_3Sn grain structure taken from transverse sections of wires unreacted and reacted under various conditions. He calculated the activation energy for grain growth as 25 $\mp$ 3 kJ/mol.

It is important to do the measurement of grain size in the bronze processed multifilamentary Nb_3Sn wires using transverse sections because

morphology of the grains varies mainly in the direction normal to the growth interface and there is no way to ensure that one can obtain radial sections in the longitudinal specimens [45, 48] . On the other hand specimen preparation from longitudinal sections is relatively easier. The author believes that SEM investigations do not have the resolution to measure the grain size especially at the early stages of growth and because it relies on fracture surfaces, it is possible to observe the grain morphology favoured by the fracture mechanism [49] , which will be misleading.

REFERENCES

1. Y.S. Hasçiçek, J. Science and Eng. Erciyes Univ., 1, 181, (1985).

2. J.B. Clark and F.N. Rhines, Trans. ASM 51, 199, (1959).

3. T. Luhman and D. Dew-Hughes, Appl. Polymer Symp. 29, 61, (1976).

4. J.P. Charlesworth et al., J. Mat. Sci. 5, 580, (1970).

5. G.V. Raynor, J. Less-Common Metals 29, 333, (1972).

6. L.D. Hartsough, J. Phys. Chem. Solids 35, 1691, (1974).

7. C.F. Old and I. Macphail, J. Mat. Sci. 4, 202, (1969).

8. R.H. Hopkins et al., Metallurgical Trans. 8A, 91, (1977).

9. D. Dew-Hughes and T. Luhman, J. Mat. Sci. 13, 1868, (1978)

10. T. Luhman, "Metallurgy of A15 conductors" in Treatise on Material, Science and Technology, Vol. 14, Edited by : T. Luhman and D. Dew-Hughes, Academic Press, N.Y. (1979), p. 221.

11. P.G. Sewman, Diffusion of Solids, McGraw-Hill, N.Y., (1963).

12. J. Crank, The Mathematics of Diffusuon, Clarendon Press, Oxford (1979).
13. M. Suenaga, "Metallurgy of Continuous Filamentary A15 Superconductors" in superconductor Materials Science, Edited by : S. Foner and B.B. Schwartz, Plenum, N.Y., (1981) p. 201
14. M. Suenaga et al., J.Appl. Phys. 45, 4049, (1974).
15. M. Suenaga et al., Appl. Phys. Lett. 25, 624, (1974).
16. K. Togano et al., J. Less-Common Metals 68, 15, (1979).
17. H.H. Farrell et al., J. Appl. Phys. 45, 4025, (1974).
18. H.H. Farrell et al., This Solid Films 25, 253, (1975).
19. D.B. Smathers and D.C. Larbalestier, Adv. in Cryo. Eng. 26, 415, (1980).
20. D.B. Smathers and D.C. Larbalestier, "Filamentary A15 Superconductors" Cryogenic Materials Series, Edited by : M. Suenaga and A.F. Clark, Plenum, N.Y. (1980), p. 143.
21. J.A. Lee et al., Colloques Int. CNDS No : 242, Physique sous champs Magnetiques Intenses" (1975) p. 87
22. D.S. Easton and D.M. Kroeger, IEEE Trans. on Magn. MAG-L5, 178, (1979).
23. Y.S. Hasçiçek, Modern Metallurgy Conference, Metals Society, Oxford. (1983)
24. J.D. Klein et al., IEEE Trans. on Magn. MAG-17, 380, (1981)
25. S. Nourbakhsh et al., J. Mat. Sci. 17, 3204, (1982).
26. R.T.P. Whitpple, Phil. Mag. 45, 1225, (1954).
27. J.C. Fisher, J. Appl. Phys. 22, 74, (1951).
28. L.G. Harrison, Trans. Faraday Soc. 57, 1191, (1961).
29. B.V. Reddi et al., Phil. Mag. 38A, 559, (1978).
30. K. Kwasnitza et al., cryogenics 20, 715, (1980).
31. J.E. Burke and D. Turnbull, Prog. Met. Phys. 3, 220, (1952).
32. P.A. Beck, Adv. Phys. 3, 245, (1954).
33. P.Cotterill and P.R. Ould, Recrystallization and Grain Growth in Metals, Surrey U.P., London, (1976).
34. G.S. Bolling and W.G. Winegard, Acta Met. 6, 283, (1958).
35. E. Nembach, J. Less-Sommon Metals 19, 359, (1969).
36. G. Zeigler et al., Phys. 31, 185, (1971).
37. J.J. Hanak and R.E. Enstrom, Proc. 10th Int. Conf. Low Temp. Phys. VINITI, Moscow, IIB, 10 (1967).
38. J.D. Livingstone and H.W. Schadler, Prog. Mat. Sci. 12, 183, (1965).
39. R.M. Scanlan et el., J. appl. Phys. 46, 2244, (1975).
40. K. Togano et al., J. Less-Common Metal 68, 15, (1979).

41. S. Okuda et al., J. Appl. Phys. 54, 289, (1983).
42. A.W. West and R.D. Rawlings J. Mat. Sci. 12, 1862, (1977).
43. C.S. Pande, "Superconductivity and Eelctron Microscopy" in Treatise on Materials Science and Technology, Vol. 14, edited by: T. Luhman and D. Dev-Hughes, Academic P., N.Y. (1979) p. 171.
44. W. Schelb, J. Mat. Sci 16, 2575, (1981).
45. Y.S. Hasçiçek et al., Proc. 10th int. Cong. Elect. Microscopy, Hamburg, 1982, 2, 203.
46. Y.S. Hasçiçek et al., Proc. 7th Int. Conf. on HVEM, Berkeley, Aug. (1983).
47. Y.S. Hasçiçek et al., J. Microscopy 131:1, 55, (1983).
48. Y.S. Hasçiçek, D. Phil. Thesis, Oxford, (1983).
49. E.D. Case et al., J. Mat. Sci. 15, 149, (1980).
50. Y.S. Hasçiçek 8th Annual Meeting of Turkish Physical Society, Ankara, (1986).